Journal of Catalysis **208,** 6–14 (2002)
doi:10.1006/jcat.2002.3550, available online at http://www.idealibrary.com on IDEAL®

Deposition and Characterization of Highly Oriented $Mg_3(VO_4)_2$ Thin-Film Catalysts

3. Effect of Exposure to Reaction Conditions

Allen G. Sault,*[,1,2] Judith A. Ruffner,† Jason E. Mudd,* and James E. Miller*

*Catalytic and Porous Materials Department and †Electronic and Optical Materials Department, Sandia National Laboratories, Albuquerque, New Mexico 87185-1349

Received June 7, 2001; revised January 24, 2002; accepted January 24, 2002

The response of oriented and amorphous thin films of magnesium orthovanadate ($Mg_3(VO_4)_2$) to reactive conditions typically encountered during oxidative dehydrogenation demonstrates that these films are excellent models for bulk $Mg_3(VO_4)_2$ powder catalysts. Fully oxidized films show little change in surface composition or chemical state upon treatment in propane, oxygen, or propane/oxygen mixtures at 673 K. As the films become more oxygen deficient, changes in both composition and chemical state are observed at the film surfaces. Reductive treatments in pure propane generally result in at least partial reduction of surface vanadium from V^{5+} to V^{3+}, and enhancement of the vanadium surface concentration. Oxidative treatments in pure oxygen reverse these effects. Behavior is highly dependent on sample history. Initial oxidation treatments reduce the magnitude of the response of the film to subsequent reduction/oxidation cycles, while initial reduction treatments increase the magnitude of the response of the film to subsequent oxidation/reduction cycles. These effects are purely kinetic in nature and can be understood from consideration of the chemical behavior of oxygen vacancies in $Mg_3(VO_4)_2$. These observations suggest that under reaction conditions magnesium vanadate surface composition may be quite dynamic, and that such dynamic variations must be considered when developing active site models for these catalysts. Comparison of the response of amorphous and (021)-oriented films provides a first indication that reactions over these catalysts may be structure sensitive.

INTRODUCTION

Oxidative dehydrogenation (ODH) offers a potential energy-saving route to formation of small alkenes such as ethene and propene. By reacting an alkane with oxygen under carefully controlled conditions, the exothermic ODH reaction offers the potential for higher conversions at temperatures lower than are possible with exothermic routes to small alkenes, such as steam cracking of natural gas liquids or nonoxidative dehydrogenation of alkanes. Because thermodynamics favor complete combustion of alkanes during ODH, selectivity becomes the major challenge in development of ODH catalysts.

ODH catalysts typically consist of complex mixed metal oxide systems that contain multiple crystalline phases, and possibly some amorphous surface phases as well. For example, magnesium vanadate catalysts, typically studied for propane ODH, can consist of as many as three different crystalline phases: $Mg_3(VO_4)_2$ (orthovanadate), $Mg_2V_2O_7$ (pyrovanadate), and MgV_2O_6 (metavanadate) (1–3). Furthermore, synergistic interactions between phases may give rise to multiphase catalysts with performance superior to that of any of the individual phases (4). Uncertainty regarding the distribution of the various phases, the relative exposed surface area of the individual phases, and the specific crystalline planes that are exposed often frustrates attempts to obtain detailed atomic-scale information regarding active site identity and properties.

We recently reported the development of a model catalyst system that simplifies the complexity inherent in working with mixed metal oxide catalysts (5, 6). Our model system consists of a thin film of magnesium orthovanadate ($Mg_3(VO_4)_2$) epitaxially deposited such that only the (021) plane of the orthorhombic crystalline lattice is exposed. The desired epitaxy is achieved by radio frequency (rf) sputter deposition of $Mg_3(VO_4)_2$ onto Au(111) surfaces. The (021) plane of the orthorhombic $Mg_3(VO_4)_2$ structure displays a pseudoclose packed geometry (Fig. 1) with an average O–O spacing nearly equal to that of Au(111), resulting in an excellent epitaxial match. By eliminating the presence of multiple crystalline phases and exposing only a single crystalline plane, this model system offers the potential for performing a more detailed study of active site properties than previously possible.

[1] To whom correspondence should be addressed. Fax: (505)845-2067. E-mail: agsault@sandia.gov.

[2] Current address: Sandia National Laboratories, MS 0807, Albuquerque, NM 87185-0807.

0021-9517/02 $35.00

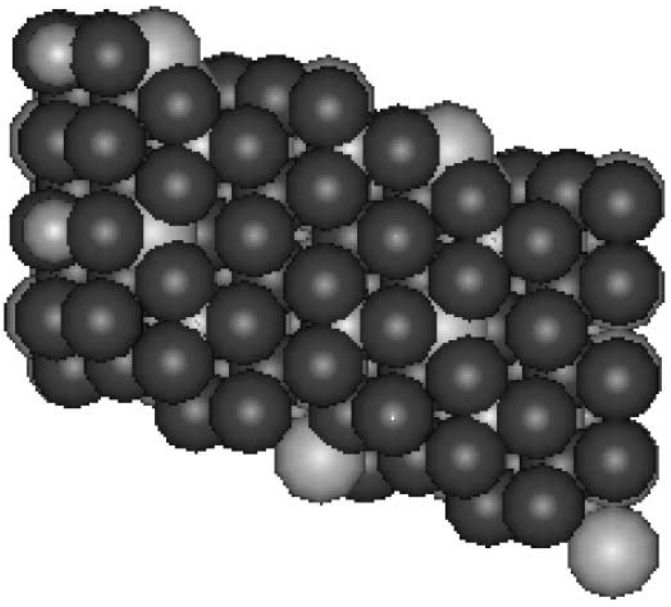

FIG. 1. Oxygen-terminated (021) surface of $Mg_3(VO_4)_2$, showing hexagonal symmetry. The dark gray spheres in the top layer are oxygen ions, while the small light gray spheres in the second layer are vanadium ions in tetrahedral sites, and the large light gray spheres in the second layer are magnesium ions in octahedral sites.

Past work (6) also shows that the oxygen content of the magnesium vanadate films can be varied substantially by controlling oxygen flow rates in the sputtering chamber during deposition. Films varying from a reduced $Mg_3V_2O_6$ phase (7), to oxygen-deficient $Mg_3(VO_4)_2$, to fully oxidized $Mg_3(VO_4)_2$ can be created (6). In this paper we report on the response of these films to treatment in oxygen, propane, and oxygen/propane mixtures at pressure and temperature conditions typically found in ODH reactors and compare the behavior of the oriented films to that of amorphous films and bulk $Mg_3(VO_4)_2$ powders. The results demonstrate that the oriented films are excellent models of bulk $Mg_3(VO_4)_2$.

EXPERIMENTAL

Full details of the film deposition process are provided elsewhere (5), so only a brief overview of the procedures are given here. As mentioned above, oriented films are prepared by deposition of $Mg_3(VO_4)_2$ onto Au(111) substrates. Polycrystalline Au(111) substrates were obtained by DC sputter deposition of 50-nm gold films onto polished Si(100) wafers covered by a 4000-Å-thick thermally grown oxide layer. $Mg_3(VO_4)_2$ films were deposited onto the Au substrates at 573 K using reactive rf sputtering from a stoichiometric ceramic target. $Mg_3(VO_4)_2$ film thickness was nominally 200 nm. Oxygen flow rate during deposition was varied from 0.0 sccm to 7.5 sccm, with the extremes of the oxygen flow rate range corresponding to deposition of $Mg_3V_2O_6$ and fully oxidized $Mg_3(VO_4)_2$, respectively (6). The oriented $Mg_3(VO_4)_2$ films are not single crystals but rather polycrystalline surfaces with random rotational orientation of the individual (021) planes. Note that the films were not calcined prior to study. Bulk syntheses of magnesium vanadates typically employ calcination at temperatures ranging from 773 to 1073 K in order to decompose precursors and promote crystallization of the material (3, 4, 8). For the thin-film synthesis, precursor decomposition is not an issue, and crystallization of the material is clearly accomplished during deposition at 573 K (5, 6).

In addition to deposition on Au(111), some films were also deposited directly onto oxidized Si wafers. Except for omission of the gold layer, deposition procedures for these films were identical to those for the (021)-oriented films. X-ray diffraction (XRD) of these films reveals the absence of any diffraction peaks other than those associated with the Si substrate. These films were therefore either amorphous or polycrystalline, with randomly oriented crystallites so small that the XRD peaks were broadened to the point of being undetectable. XRD was performed using standard θ-2θ X-ray diffraction on a Siemens D-500 XRD.

For clarity, we adopt the following nomenclature. Oriented samples are designated MgVO-o($x \cdot y$), where the "o" indicates an oriented film, and $x \cdot y$ indicates the oxygen flow rate (in sccm) during deposition (e.g., 0.0, 0.3, 1.0, etc.). Amorphous films are designated MgVO-a($x \cdot y$), where the "a" indicates an amorphous film and $x \cdot y$ indicates the oxygen flow rate. The use of the "a" designation is solely designed to distinguish these films from the (021)-oriented films, but the reader should bear in mind that we cannot preclude the possibility that the films are actually polycrystalline.

In addition to the thin-film samples, a powder sample of $Mg_3(VO_4)_2$ was prepared using the citrate method (3, 9). A transparent solution of $Mg(NO_3)_2$ and NH_4VO_3 in the proper stoichiometric ratio was treated with citric acid in an amount to give a 10% molar excess of anions over cations. The solution was evaporated in a rotovap at 313 K to obtain a viscous material and then dried at 253–263 K to obtain a solid. The dry solid was decomposed in air at 653 K for 18 h and then calcined at 823 K for 6 h. The resulting powder possessed a surface area of 25.5 m^2/g and gave the powder XRD pattern expected for $Mg_3(VO_4)_2$ with no detectable impurities. This sample provided a standard against which the thin-film samples were compared to determine their suitability as models of bulk $Mg_3(VO_4)_2$ catalysts.

Film reactivity was analyzed by a combination of X-ray photoelectron spectroscopy (XPS), XRD, and Fourier transform infrared (FTIR) spectroscopy. XPS was performed using a VG Microtech Clam 2 operated at an analyzer resolution of 1.0 eV, with excitation provided by a VG Microtech XR3 Al Kα X-ray source. The XPS

system is housed in a UHV chamber coupled to an atmospheric pressure reactor, which allowed treatment of the films in reactive environments typical of those found during oxidative dehydrogenation, followed by transfer to UHV without intervening exposure to air. Samples were prepared by cleaving the Si wafers to form 13×7 mm pieces, which were then mounted between copper clamps on each side of the sample holder. Heating was accomplished by passing current directly through the samples. Temperature was measured using a Cr–Al thermocouple spot welded to a small Ta clip that was press-fit to the top edge of the sample.

Treatment in propane/oxygen mixtures involved isolation of the sample in the reactor and sequential introduction of propane and oxygen to pressures of 100 and 50 Torr, respectively. The 2:1 propane:oxygen ratio is stoichiometric for the ODH reaction and the total reactant pressure approximates that used in earlier studies of propane ODH in our laboratory (10). The sample was heated to the desired temperature for the desired time in the reaction mixture and then cooled to room temperature while simultaneously being evacuated from the reactor. The sample was then transferred into the UHV chamber for XPS analysis. A similar procedure was employed for treatment in pure oxygen. Treatment in pure propane differed in that following the treatment the reactor was evacuated while holding the sample at the treatment temperature. With this procedure, buildup of carbonaceous residue (which can interfere with XPS measurements) is minimized since weakly bound carbon-containing species desorb during evacuation. Because heating in vacuum was found to be mildly reducing, this procedure was avoided during treatment in pure oxygen or oxygen/propane mixtures in order to minimize changes in the chemical state of the surface during evacuation. Propane (Matheson, Research Grade, 99.97%) and oxygen (Matheson, Research Grade, 99.998%) were used as received without further purification.

Identification of V oxidation states by XPS has been discussed elsewhere (3, 6). The $2p_{3/2}$ binding energy of V^{5+} is generally agreed to be between 517.1 and 517.6 eV, with the latter value being used in this work. We also observed a second V oxidation state with a binding energy of roughly 515.5 eV in reduced samples. In an earlier paper (6), we argued for assignment of this peak to V^{3+}, although others have assigned this peak to V^{4+} (3). For the purposes of this paper, it is sufficient to state that this peak corresponds to a reduced form of V, without specifying the exact oxidation state. For fully oxidized films, binding energies were referenced to the V $2p_{3/2}$ peak at 517.6 eV, corresponding to V^{5+}. Fully oxidized films were identified by the presence of a sharp, symmetrical V $2p_{3/2}$ peak 13.0 ± 0.1 eV below the O 1s peak. Only fully or nearly fully oxidized films exhibit charging during XPS. Partially reduced or oxygen-deficient films generally display a broad V $2p_{3/2}$ peak consisting of both V^{5+} and reduced V. These films have a relatively high electrical conductivity and do not exhibit any charging during XPS.

Quantitation of the XPS results was performed using published sensitivity factors (11) and integrated areas under the Mg 2s, Mg 2p, and V 3p XPS peaks. These peaks were chosen rather than the more intense Mg 1s and V 2p peaks since these latter photoelectrons (particularly the Mg 1s peak) have relatively short inelastic mean free paths (IMFP) and are therefore subject to severe attenuation by adventitious carbonaceous overlayers invariably found on samples exposed to air or subjected to treatment in propane-containing environments. The Mg 2s, Mg 2p, and V 3p photoelectrons all have relatively long IMFPs and are therefore less susceptible to attenuation. Furthermore, these photoelectrons all have very similar kinetic energies (~1380–1430 eV), so that any attenuation that does occur is of similar magnitude for all of the peaks, and the relative areas of the peaks are unaffected.

A Nicolet 20SXB Fourier transform infrared spectrometer equipped with a SpectraTech COLLECTOR™ diffuse reflectance accessory was used to obtain FTIR spectra of the films. Although this accessory is not designed for specular reflectance measurements, we have found that high-quality reflectance spectra can be obtained provided the angle of incidence is adjusted so that the IR beam penetrates the film and is reflected off the underlying gold layer rather than off the surface of the $Mg_3(VO_4)_2$ films. Samples were mounted by placing a small piece of the coated Si wafer on top of the diffuse reflectance sample cup and adjusting the optics to maximize signal. Background spectra were obtained from an oxidized Si wafer coated with a 50-nm Au film, deposited in a fashion identical to those used as substrates for the $Mg_3(VO_4)_2$ films. More extensive IR measurements and analysis of these films was given in earlier work (6). An attempt was made to obtain FTIR spectra of the amorphous films in a manner similar to that used for the oriented films. In this case background spectra were taken directly from a polished, oxidized Si wafer. Unfortunately, the randomly oriented films displayed very weak absorption at the wavelengths of interest, and signal-to-noise ratios were not sufficient to allow meaningful data interpretation. An FTIR spectrum of the $Mg_3(VO_4)_2$ powder was obtained by mixing the powder with ground KBr to give 5 wt% orthovanadate and then filling the sample cup of the FTIR diffuse reflectance accessory with the mixture.

RESULTS AND DISCUSSION

Oriented Films

A major issue in using model systems to represent real catalysts is whether the chemical behavior of the simplified model system is sufficiently close to that of the real catalyst. In order to address this question we subjected the

thin-film model catalysts to treatments known to induce chemical and structural changes in the bulk orthovanadate. One treatment involves severe reduction of $Mg_3(VO_4)_2$. Wang *et al.* (7) showed that treatment of $Mg_3(VO_4)_2$ in hydrogen at 833 K for 60 h converts the orthorhombic orthovanadate into cubic $Mg_3V_2O_6$. Lubin and Rittershaus (12) also affected this conversion, reporting only the formation of a cubic orthovanadate phase. Finally, Burrows *et al.* (8) reported formation of this phase during reaction in a propane-rich mixture at 773 K, though they identify the phase as a cubic spinel, MgV_2O_4. Because Wang *et al.* performed a detailed structural analysis of the phase, we favor their proposed stoichiometry over that of Burrows *et al.* Nonetheless, it is clear that a reduced cubic phase containing only V^{3+} is formed upon treatment of $Mg_3(VO_4)_2$ under reducing conditions.

Accordingly, we subjected a 200-nm MgVO-o(2.5) film to 100 Torr of propane at 773 K for 2 h. This film is known to be initially somewhat oxygen deficient (6). As shown below, this oxygen deficiency enhances the response of the film relative to that of fully oxidized films and likely eases the transition to the reduced cubic phase. Figure 2 demonstrates quantitative reduction of V^{5+} in the near-surface region of the film following this treatment. No evidence for V^{5+} remains by XPS after the propane treatment. Furthermore, qualitative agreement is obtained between the FTIR spectra of the reduced film (Fig. 3b) and that of a film deposited in the absence of oxygen and previously shown to contain the reduced $Mg_3V_2O_6$ phase (Fig. 3d) (6). The loss of intensity in the 900- to 1000-cm^{-1} region, attributed to VO_4 tetrahedra, supports the formation of the $Mg_3V_2O_6$ phase since VO_4 tetrahedra are present in $Mg_3(VO_4)_2$, but not in $Mg_3V_2O_6$ (6, 7). The quantitative differences between Figs. 3b and 3d can be explained by different amounts of residual $Mg_3(VO_4)_2$ in the films, as well as a (100)

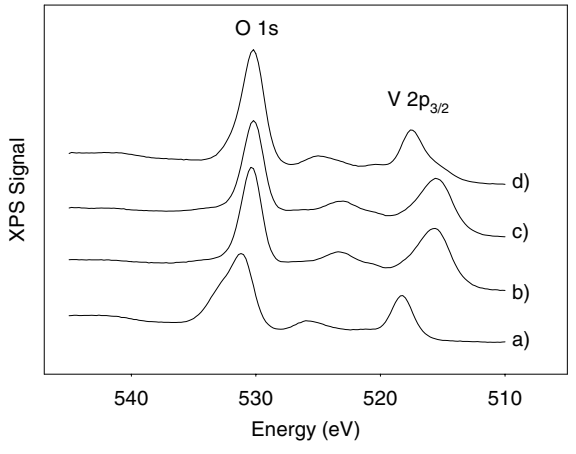

FIG. 2. XPS of the V 2p and O 1s regions of a 200-nm $Mg_3(VO_4)_2$ film prepared with 2.5 sccm oxygen: (a) as-prepared film, (b) treatment in 100 Torr of propane for 1 h at 773 K, (c) treatment in 100 Torr of propane for 2 h at 773 K, and (d) reoxidation in 50 Torr of oxygen at 673 K for 1 h.

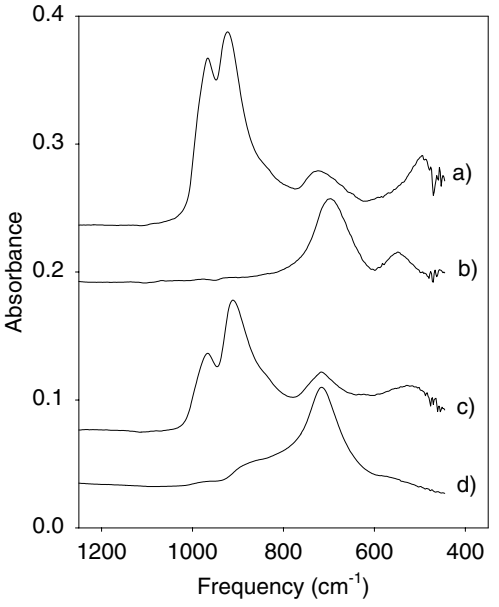

FIG. 3. FTIR spectra of a 200-nm $Mg_3(VO_4)_2$ film prepared with 2.5 sccm oxygen: (a) as-prepared film, (b) after treatment in 100 Torr of propane for 2 h at 773 K, and (c) after reoxidation in 50 Torr of oxygen at 673 K for 1 h. Shown for comparison in (d) is the spectrum of a 200-nm film prepared in the absence of oxygen and which is known to contain $Mg_3V_2O_6$ (6).

orientation for the film deposited in the absence of oxygen (6) vs a (111) orientation for the film prepared by reduction of $Mg_3(VO_4)_2$ (5). These two pieces of evidence, coupled with XRD data reported earlier (5) showing the appearance of diffraction peaks from $Mg_3V_2O_6$ upon reduction, argues strongly for nearly complete conversion of the $Mg_3(VO_4)_2$ film to $Mg_3V_2O_6$. Subsequent treatment of the reduced film in 50 Torr of O_2 at 773 K reverses the transformation, resulting in disappearance of the XRD peaks due to $Mg_3V_2O_6$, conversion of V^{3+} to V^{5+} (Fig. 2) and in restoration of the original FTIR spectrum of the oriented $Mg_3(VO_4)_2$ film (Fig. 3). Burrows *et al.* (8) also report that the conversion is reversible, though it becomes more difficult with the extent of ordering of the cubic phase. Altogether, it appears that the reduction behavior of the oriented $Mg_3(VO_4)_2$ film closely approximates that of bulk $Mg_3(VO_4)_2$ powders, providing further evidence that the $Mg_3(VO_4)_2$ films are good models of bulk $Mg_3(VO_4)_2$.

We next investigated the behavior of the oriented $Mg_3(VO_4)_2$ films under less severe reaction conditions. Specifically, we looked at the response of the films to treatment under stoichiometric reaction mixtures (2 : 1 mixture of propane and oxygen) at 673 and 773 K, and in both pure oxygen and pure propane at 673 K. Figure 4 shows the V 2p XPS of the MgVO-o(2.5) film as a function of cyclic reduction/oxidation treatments at 673 K. At this temperature only partial reduction of surface vanadium occurs during treatment in propane, resulting in a shoulder at 515.5 eV

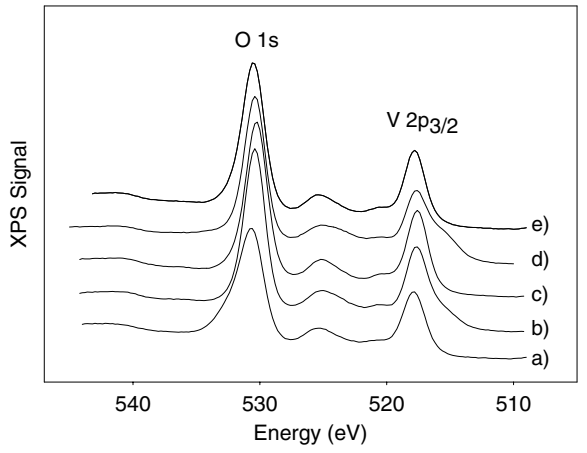

FIG. 4. XPS of MgVO-o(2.5) film following cyclic reduction/oxidation treatments: (a) as-prepared film; (b) 100 Torr of propane, 673 K, 1 h; (c) 50 Torr of oxygen, 673 K, 0.5 h; (d) 100 Torr of propane, 673 K, 1 h; and (e) 50 Torr of oxygen, 673 K, 0.5 h.

on the low-binding-energy side of the V $2p_{3/2}$ peak. Subsequent oxidation reverses the reduction restoring the surface V to the +5 oxidation state. Repeated cycling reproducibly results in partial conversion to reduced surface V during reduction, followed by reoxidation to V^{5+} during oxygen treatments. This reversible redox behavior is entirely consistent with the well-known Mars–Van Krevelen mechanism for oxidative dehydrogenation, whereby oxygen from the crystalline lattice of the catalyst is extracted by propane to form oxidation products, followed by replenishment of the oxygen vacancy, either by direct adsorption of oxygen from the gas phase at the vacancy site or by adsorption of gas-phase oxygen at a different site followed by diffusion of oxygen ions through the catalyst to the oxygen vacancy.

In Fig. 5, the effects of various treatments on the surface composition of the MgVO-o(5.0) film are shown. The initial surface composition of the film is identical to the bulk stoichiometry of $Mg_3(VO_4)_2$ within the measurement error of ±5%. A casual inspection of the figure clearly reveals two facts regarding the effects of reactive environments. First, surface composition can change substantially as a result of exposure to reactive environments. V/Mg surface ratios as low as 0.47 and as high as 0.78 were observed for this sample. More extreme values have been observed for other samples (see below). These deviations from the bulk stoichiometric ratio show that the surface compositions of $Mg_3(VO_4)_2$ ODH catalysts are not constant during reaction and may in fact differ substantially from the bulk composition. Second, the sample response to a given treatment is highly dependent on previous history. For example, exposure to oxygen at 673 K results in little or no change in surface composition when applied to a fresh sample, but results in a large decrease in V surface content when applied to a sample previously treated in propane/oxygen mixtures at 673 and 773 K.

Not apparent in Fig. 5 is a direct correlation between changes in surface composition and V oxidation state. Increases in the V/Mg surface ratio are invariably accompanied by reduction of surface V, with the extent of reduction roughly correlating with the percentage increase in the V/Mg ratio. Decreases in V/Mg ratios are invariably accompanied by oxidation of surface V. Applying this correlation leads to the conclusion that stoichiometric propane/oxygen mixtures change from oxidizing to reducing as the temperature increases from 673 to 773 K. This result can be understood by postulating that the reaction of propane with lattice oxygen to produce oxygen vacancies and reduced V, and the reoxidation of V, are two independent reactions with different activation energies. If reoxidation of vacancies has a lower apparent activation energy than the reaction of propane with lattice oxygen, then at low temperatures reoxidation would be faster, but at high temperatures reaction with propane would be faster.

The preferential segregation of vanadium to the surface under reducing conditions is analogous to the observed spreading of reducible oxides on supported metal particles that occurs as a result of strong metal–support interactions (SMSI) (13). The SMSI phenomenon arises from the apparent ability of reduced forms of oxides, such as titania, to wet metal surfaces. Under strong reducing conditions titania is partially reduced and spreads over the surface of titania-supported metal particles. Upon reoxidation the titania can no longer wet the surface of the metal particles, resulting in either agglomerization of the titania into small, nonwetting patches on the metal surfaces or diffusion of

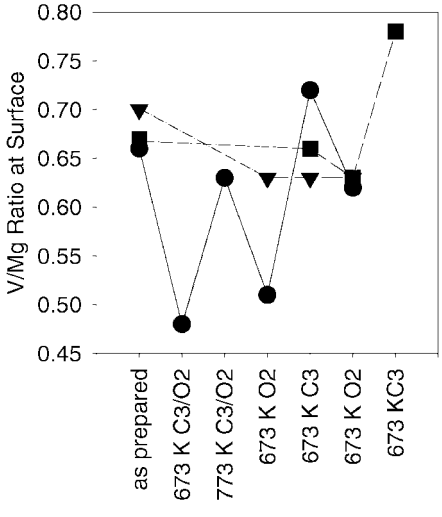

FIG. 5. Effect of reactive treatments on the surface composition of the MgVO-o(5.0) film. Propane/oxygen treatments were performed for 1 h in the presence of 50 Torr of O_2 and 100 Torr of propane. Oxygen treatments were performed under 50 Torr of O_2, while propane treatments were performed under 100 Torr of propane. Treatment temperatures are indicated in the figure. ●, Treatment in propane/oxygen mixtures followed by oxidation/reduction cycles; ▲, oxidation/reduction cycles beginning with oxidation; ■, oxidation/reduction cycles beginning with reduction.

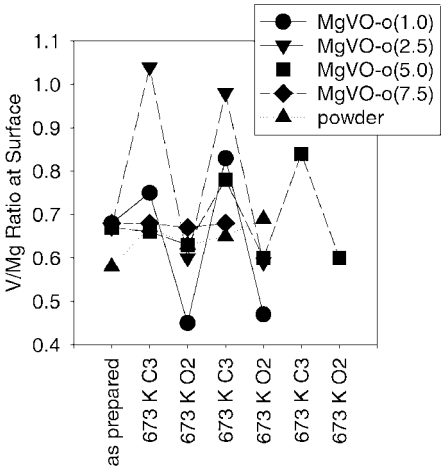

FIG. 6. Effect of reduction/oxidation cycles on the surface composition of oriented films as a function of oxygen flow rate during deposition. Reduction treatments are at 673 K under 100 Torr of propane for 1 h, while oxidation treatments are at 673 K under 50 Torr of oxygen for 0.5 h. Initial treatment is reduction.

the titania off the metal particle surface and back into the support. Although the analogy to SMSI is strained by the absence of metallic particles in these experiments, similar arguments nevertheless provide a plausible explanation for the increases in V/Mg ratios observed after reduction of the $Mg_3(VO_4)_2$ films. V^{5+} is partially reduced and becomes capable of wetting the $Mg_3(VO_4)_2$ surface. Upon reoxidation, V is converted back into V^{5+}, which either agglomerates into patches of V_2O_5 on the surface or diffuses back into the bulk of the $Mg_3(VO_4)_2$ film.

Figures 6 and 7 demonstrate the changes in surface composition resulting from reduction/oxidation cycles for films deposited with a range of oxygen flow rates. Figure 6 gives results when the initial treatment is reduction, while Fig. 7 gives results when the initial treatment is oxidation. For reasons that will become apparent, we first discuss results for oxygen flow rates of 2.5 sccm or greater and then discuss results for lower oxygen flow rates separately.

For oxygen flow rates of 2.5 sccm or greater, it is apparent that the amount of V detected at the surface following reduction increases as oxygen flow rate during deposition decreases. Also apparent is the fact that films subjected to an initial reduction treatment (Fig. 6) generally display greater variations in surface composition than those subjected to an initial oxidation treatment (Fig. 7). For example, for sample MgVO-o(5.0) the initial reduction/oxidation cycle has little effect on surface composition but subsequent cycles show increasing oscillations in the V/Mg ratio (Fig. 6). When the initial treatment is oxidizing (Fig. 7), this sample never displays any significant variation in the V/Mg ratio, even after the third oxidation treatment.

Included in Figs. 6 and 7 are results for the $Mg_3(VO_4)_2$ powder. Except for a slight V deficiency on the surface of the as-prepared powder (also noted by Carrazán *et al.* (4)), the behavior of the MgVO-o(7.5) film is identical to that of the powder, suggesting that this film is fully oxidized and therefore an excellent model for bulk $Mg_3(VO_4)_2$. The behavior of the MgVO-o(5.0) film diverges from that of the powder when subjected to an initial reduction treatment, indicating that this film is not fully oxidized.

The increasing amounts of reduced V formed at the surface with decreasing oxygen flow rate during deposition, as well as the history-dependent behavior of the samples, can be understood from consideration of the behavior of oxygen vacancies in $Mg_3(VO_4)_2$. Oxygen vacancies are clearly mobile in these materials, as evidenced by electrical conductivity measurements (14). This oxygen vacancy mobility is widely believed to be key to the catalytic activity of mixed metal oxides, since it allow vacancies formed by reaction with alkanes to diffuse into the bulk and thereby eliminate oxygen vacancies at the surface. This behavior is likely responsible for the observation that ODH reactions occur on mixed metal oxides even in the absence of gas-phase oxygen, with reaction rates declining only slightly even after an amount of oxygen equivalent to 50% of a monolayer has been consumed (1).

With this understanding, we can postulate that the increase in V reduction and concentration at the surfaces of the films with decreasing oxygen flow rate is related to a competition between oxygen vacancy formation at the surface and diffusion of these vacancies into the bulk. Films deposited with high oxygen flow rates initially contain few oxygen vacancies in the bulk or at the surface. Upon reduction, any oxygen vacancies created at the surface rapidly diffuse into the bulk, leaving the surface essentially fully

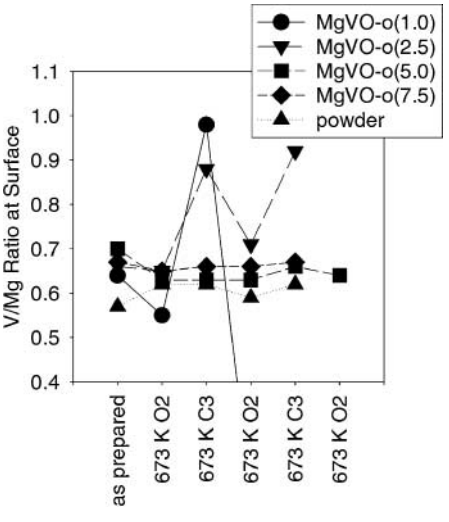

FIG. 7. Effect of oxidation/reduction cycles on the surface composition of oriented films as a function of oxygen flow rate during deposition. Reduction treatments are at 673 K under 100 Torr of propane for 1 h, while oxidation treatments are at 673 K under 50 Torr of oxygen for 0.5 h. Initial treatment is oxidation.

oxidized. Films deposited with low oxygen flow rates contain relatively high concentrations of oxygen vacancies at both the surface and in the bulk, but exposure to air following deposition fills oxygen vacancies near the surface, resulting in a fully oxidized surface (6). Upon reduction of such samples, oxygen vacancies are created at the surface, but because of the high vacancy concentration in the bulk there is no concentration gradient to drive diffusion of vacancies away from the surface. Instead, the vacancies remain at the surface, where they spread over the surface and form the reduced V phase detected by XPS.

The history-dependent behavior of the samples is also explicable in terms of initial oxygen vacancy concentration. For all samples initial oxidation results in at least partial filling of oxygen vacancies formed during film deposition. As a result, following a subsequent reduction the film is better able to accommodate surface oxygen vacancies by diffusion into the bulk, decreasing the amount of reduced V observed by XPS. Conversely, initial reduction results in increased concentrations of oxygen vacancies and segregation of reduced V to the surface. These changes are not completely reversed during a subsequent oxidizing treatment.

These effects must be purely kinetic in nature and not related to equilibrium considerations. In an attempt to demonstrate the kinetic limitations, selected samples were subjected to reduction and oxidation cycles with treatment times doubled over those used to obtain the data in Figs. 6 and 7. No significant changes in surface composition were observed as a result of the extended treatment times. This result can be explained by assuming that oxygen-deficient films are in a thermodynamically unstable or metastable state following deposition. Depending upon the initial treatment, the films are converted into one of two more stable states, corresponding to a fully oxidized $Mg_3(VO_4)_2$ film (favored by initial oxidation) or an oxygen-deficient $Mg_3(VO_4)_2$ film with reduced V species segregated to the surface (favored by initial reduction). Within this hypothesis, there must be a large kinetic barrier to conversion between the states. The MgVO-o(5.0) film provides an excellent example of bifurcation between the two states. This film is known to be only slightly oxygen deficient (6). Initial oxidation fills most of the oxygen vacancies and drives the film toward the fully oxidized state, which displays no significant response to subsequent reduction/oxidation treatments (Fig. 7). Initial reduction results in minor segregation of reduced V to the surface, but the extent of segregation increases with continued oxidation/reduction cycles as the sample is driven into the oxygen-deficient state (Fig. 6).

It is important to note that the amount of reduced vanadium at the surface following reduction is not necessarily an indicator of catalytic activity for ODH. Experiments with bulk orthovanadate powder indicate that reaction rates are highest with fully oxidized orthovanadate (1). The failure to observe reduced vanadium following reduction of fully oxidized films is the result of rapid replenishment of surface oxygen by diffusion of vacancies into the bulk, and not the result of low activity. It is for this reason that we have been careful to distinguish between the response of the films to exposure to reactive conditions and the reactivity or catalytic activity of the films.

The above discussion is only valid when the film structure is that of $Mg_3(VO_4)_2$ containing a limited concentration of oxygen vacancies. When the oxygen flow rate during deposition falls below a critical value, formation of the reduced $Mg_3V_2O_6$ phase begins and the film can no longer be considered to have the oxygen-deficient $Mg_3(VO_4)_2$ structure assumed above. In this case the oxygen deficiency of the film is accommodated not by formation of oxygen vacancies in $Mg_3(VO_4)_2$ but by formation of $Mg_3V_2O_6$, which likely exhibits reduction/oxidation behavior completely different from that of orthovanadate. This consideration explains the apparent anomalous behavior of the MgVO-o(1.0) sample seen in Fig. 6. While $Mg_3V_2O_6$ formation does not become apparent by XRD until oxygen flow rates fall below 1.0 sccm, it is likely that some $Mg_3V_2O_6$ is formed even at 1.0 sccm, though not to an extent detectable by XRD.

The large variations in surface composition with reactive treatment for the oxygen-deficient films does not indicate that the films behave differently from bulk $Mg_3(VO_4)_2$ powder. Because the powder synthesis involves a high-temperature (823 K) calcination step, it is expected that the powder is fully oxidized. For this reason, the powder should only be compared to the fully oxidized MgVO-o(7.5) and MgVO-a(7.5) films, which show only minor variations in surface composition following reactive treatments. The conclusion is that the films and the powder show very similar behavior, and that the films are excellent models for bulk orthovanadate catalysts. The more interesting behavior of the oxygen-deficient films provides key insights into the reactive properties of these materials but is not quantitatively indicative of the behavior of bulk orthovanadate powder.

Amorphous Films

Figures 8 and 9 compare the behavior of the oriented films with that of the amorphous films. For the fully oxidized films (7.5 sccm) there is no significant difference between the oriented and the amorphous films; however, as the oxygen deficiency of the films increases, the amorphous films display much smaller extents of surface V reduction and V segregation than the oriented films. In fact, for the amorphous films decreasing the oxygen flow rate from 7.5 to 2.5 sccm appears to have no effect on the response of the films to oxidation and reduction treatments.

This difference in behavior of the amorphous and oriented films provides possible evidence for structure sensitivity in $Mg_3(VO_4)_2$ ODH catalysts. The (021) surfaces of the oriented films display far greater variations in surface composition during reduction/oxidation cycles than

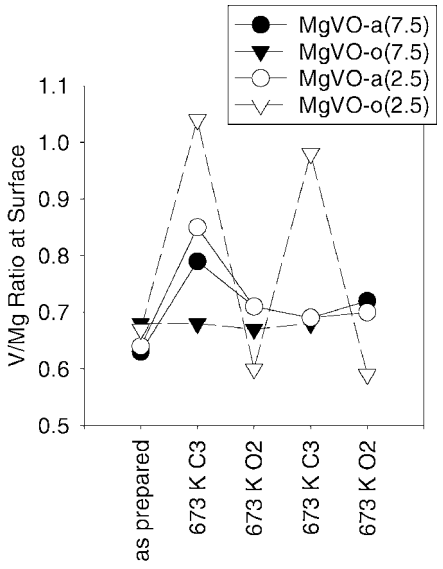

FIG. 8. Comparison of oriented and amorphous film surface composition during reduction/oxidation cycles. Reduction treatments are at 673 K under 100 Torr of propane for 1 h, while oxidation treatments are at 673 K under 50 Torr of oxygen for 0.5 h. Initial treatment is reduction.

the surfaces of the amorphous films, which presumably consist of a thermodynamically weighted mixture of various crystalline planes. One possible explanation for the structure sensitivity is that transport of oxygen vacancies from the surface to the bulk is slower at (021) surfaces than at other surfaces. As a result, the amorphous films are able to accommodate oxygen vacancies through diffusion into the bulk at vacancy concentrations that result in accommodation via V reduction and spreading on the (021) surface.

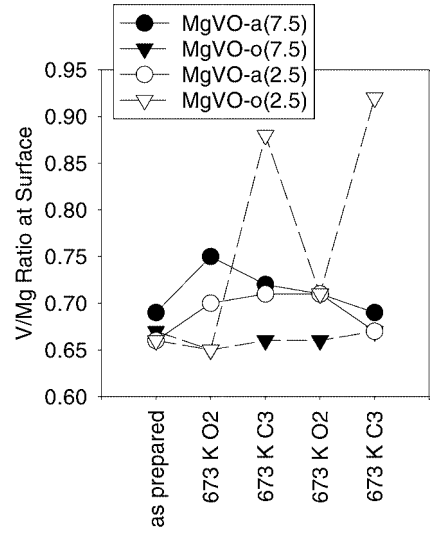

FIG. 9. Comparison of oriented and amorphous film surface composition during oxidation/reduction cycles. Reduction treatments are at 673 K under 100 Torr of propane for 1 h, while oxidation treatments are at 673 K under 50 Torr of oxygen for 0.5 h. Initial treatment is oxidation.

The most definitive demonstration of structure sensitivity would involve tests of the catalytic activity of the amorphous and oriented films. Extensive efforts were made to measure the ODH activity of the $Mg_3(VO_4)_2$ films in a flow reactor successfully used to test high-surface-area powdered propane ODH catalysts (10). Unfortunately, the extremely low surface area of the films, coupled with a large void volume which promoted homogeneous reactions, prevented meaningful measurement of catalytic activity. Future experiments are planned to measure catalytic activity in a batch reactor where extended reaction times will allow measurable conversions to be achieved. These experiments should allow conclusive confirmation or refutation of the structure sensitivity of $Mg_3(VO_4)_2$ catalysts for ODH.

CONCLUSIONS

Tests of the behavior of $Mg_3(VO_4)_2$ films under reaction conditions approximating those typically found during propane ODH demonstrate the effects of oxygen vacancies and film surface structure on film reactivity. For (021)-oriented films the presence of oxygen vacancies in the bulk decreases the rate at which surface vacancies, formed by reaction with propane, diffuse into the bulk. As a result surface oxygen vacancies are more likely to be accommodated by formation of reduced V at the surface, accompanied by spreading of a reduced V phase across the surface. This process appears to be at least partially reversible upon oxidation of the surface, resulting in reoxidation of V to the +5 state and either agglomeration of the V into V_2O_5 or reincorporation of V back into the bulk. These observations suggest that under reaction conditions magnesium vanadate surface composition may be quite dynamic, and that such dynamic variations must be considered when developing active site models for these catalysts.

Chemical behavior of the (021) surface is highly history dependent. Initial oxidation of the films tends to eliminate oxygen vacancies and decrease the likelihood that subsequent reduction will result in formation of reduced V at the surface. Initial reduction of the films increases oxygen vacancy concentration, promoting formation of the reduced V phase and decreasing the likelihood that subsequent oxidation will restore the initial state of the film. Fully oxidized films, containing few oxygen vacancies, display behavior that closely resembles that of $Mg_3(VO_4)_2$ powders, confirming that the films are good models for ODH catalysts.

Comparison of (021)-oriented films with amorphous films provides the first reported evidence for structure sensitivity in these materials. The amorphous films are far less likely to exhibit reduced V at the surface than the (021)-oriented films. This difference may be attributed to higher rates of diffusion of oxygen vacancies from the surface into the bulk on the amorphous films.

ACKNOWLEDGMENTS

The authors thank Amitesh Maiti of Molecular Simulations, Inc., for providing the $Mg_3(VO_4)_2$ (021) image shown in Fig. 1, and Timothy J. Gardner of Sandia National Laboratories for helpful comments on the manuscript. This work is supported by the U.S. Department of Energy under Contract DE-AC04-94AL85000. Sandia is a multiprogram laboratory operated by Sandia Corporation, a Lockheed Martin Company, for the United States Department of Energy.

REFERENCES

1. Kung, H. H., *Adv. Catal.* **40**, 1 (1994).
2. Siew Hew Sam, D., Soenen, V., and Volta, J. C., *J. Catal.* **123**, 417 (1990).
3. Gao, X., Ruiz, P., Guo, X., and Delmon, B., *J. Catal.* **148**, 56 (1994).
4. Carrazán, S. R. G., Peres, C., Bernard, J. P., Ruwet, M., Ruiz, P., and Delmon, B., *J. Catal.* **158**, 452 (1996).
5. Ruffner, J. A., Sault, A. G., Rodriquez, M. M., and Tissot, R. G., Jr., *J. Vac. Sci. Technol. A* **18**, 1928 (2000).
6. Sault, A. G., Ruffner, J. A., and Mudd, J. E., *Catal. Lett.* **76**, 177 (2001).
7. Wang, X., Zhang, H., Sinkler, W., Poeppelmeier, K. R., and Marks, L. D., *J. Alloys Cmpd.* **270**, 88 (1998).
8. Burrows, A., Kiely, C. J., Perregaard, J., Højlund-Nielsen, P. E., Vorbeck, G., Calvino, J. J., and López-Cartes, C., *Catal. Lett.* **57**, 121 (1999).
9. Courty, Ph., Ajot, H., Marcilly, Ch., and Delmon, B., *Powder Technol.* **7**, 21 (1973).
10. Miller, J. E., Jackson, N. B., Evans, L., Sault, A. G., and Gonzales, M. M., *Catal. Lett.* **58**, 147 (1999).
11. Wagner, C. D., Davis, L. E., Zeller, M. V., Taylor, J. A., Raymond, R. M., and Gale, L. H., *Surf. Interface Anal.* **3**, 211 (1981).
12. PDF card 19-0778, JCPDS—International Center for Diffraction Data, Newtown Square, PA.
13. Stevenson, S. A., Dumesic, J. A., Baker, R. T. K., and Ruckenstein, E., "Metal-Support Interactions in Catalysis, Sintering, and Redispersion." Van Nostrand Reinhold, New York, 1987.
14. Pantazidis, A., Burrows, A., Kiely, C. J., and Miradatos, C., *J. Catal.* **177**, 325 (1998).